Host–Guest Systems

DOI: 10.1002/ange.201408491

Switchable Guest Molecular Dynamics in a Perovskite-Like Coordination Polymer toward Sensitive Thermoresponsive Dielectric Materials**

Zi-Yi Du, Ting-Ting Xu, Bo Huang, Yu-Jun Su, Wei Xue, Chun-Ting He, Wei-Xiong Zhang, and Xiao-Ming Chen*

Abstract: *A new perovskite-like coordination polymer $[(CH_3)_2NH_2][Cd(N_3)_3]$ is reported which undergoes a reversible ferroelastic phase transition. This transition is due to varied modes of motion of the $[(CH_3)_2NH_2]^+$ guest accompanied by a synergistic deformation of the $[Cd(N_3)_3]^-$ framework. The unusual two-staged switchable dielectric relaxation reveals the molecular dynamics of the polar cation guest, which are well controlled by the variable confined space of the host framework. As the material switches from the ferroelastic phase to the paraelastic phase, a remarkable increase of the rotational energy barrier is detected. As a result, upon heating at low temperature, this compound shows a notable change from a low to a high dielectric state in the ferroelastic phase. This thermoresponsive host–guest system may serve as a model compound for the development of sensitive thermoresponsive dielectric materials and may be key to understanding and modulating molecular/ionic dynamics of guest molecules in confined space.*

Host–guest systems that can respond to external stimuli, such as temperature, pressure, light, pH, or concentration, have attracted much attention because of their theoretical significance in multiple disciplines and their potential application in a wide variety of fields.[1–8] Among various types of stimuli-responsive host–guest systems, coordination polymers (CPs) which mimic the inorganic ABO_3-type perovskite structure, as one type of CP-based inclusion compound, have potentially promising applications in modern optoelectronic materials, such as dielectric, ferroelectric, and base materials for high-efficiency photovoltaics.[9–16] These perovskite-like CPs, with inclusion of guest cations within the well-matched cage-like host frameworks, can undergo reversible structural phase transitions upon thermal stimulus, which can often lead to a change or a switch of the related physical properties. Additionally, the metal species, bridging ligand, and guest cation component of these systems have designable and tunable characteristics. In combination, perovskite-like CPs may serve as a unique host–guest model to understand and modulate the molecular dynamics of the guest cations in the variable confined space constructed by the host frameworks.

To date, the ligands commonly employed for the construction of perovskite-like CPs have contained mostly the monoatomic I^-, diatomic CN^-, and triatomic $HCOO^-$ ions. It was found that the guest cations, rather than the host frameworks, play a key role in their structural phase transitions. However, compared with the host frameworks constructed by the above-mentioned bridging ligands, and in particular the curved $HCOO^-$ ion, those constructed using a rodlike N_3^- spacer can play a more important role to induce the structural transitions. The azido coordination framework has more flexible and deformable characteristics, as indicated by the structural analyses from our recent[17] and other related reports,[18,19] and can mainly be ascribed to the longer length of the azido bridge between two metal nodes. As a result, the angle between the N_3^- rod and a line connected by its two metal nodes often drastically deviates from the ideal zero degrees.

Based on these findings, a flexible and deformable azido coordination framework of this type using a metal species with a large ionic radius and an easily distorted coordination environment is employed to construct a variable confined space. This system is used to investigate the thermal motion and especially the polarization behavior of cation guests with a strong dipole moment within it. We anticipated that a host–guest system of this type might act as a sensitive thermally responsive dielectric material. With this goal in mind, herein we present a new perovskite-like azido CP $[(CH_3)_2NH_2][Cd(N_3)_3]$ (**1**) with dimethyl ammonium as the polar cationic guest. This CP is a rare example of a CP-based ferroelastic inclusion compound which exhibits distinguishable dielectric relaxations in both the ferroelastic and paraelastic phases, and a remarkable dielectric switch during the phase transition. Its synthesis, crystal structure, phase transition, and dielectric properties are described, as well as the inherent guest molecular dynamics uncovered by variable-temperature dielectric measurements.

[*] Dr. Z.-Y. Du, B. Huang, Y.-J. Su, Dr. W. Xue, C.-T. He, Dr. W.-X. Zhang, Prof. Dr. X.-M. Chen
MOE Key Laboratory of Bioinorganic and Synthetic Chemistry
School of Chemistry and Chemical Engineering
Sun Yat-Sen University, Guangzhou 510275 (China)
E-mail: zhangwx6@mail.sysu.edu.cn
Dr. Z.-Y. Du, T.-T. Xu
College of Chemistry and Chemical Engineering
Gannan Normal University, Ganzhou 341000 (China)

[**] This work was supported by the NSFC (21290173, 21301198, and 91422300), the 973 Project (2012CB821706), and NSF of Guangdong (S2012030006240). W.-X.Z. is grateful for initial funding from "100 Talents Program of SYSU". Z.-Y.D. is thankful to the NSFC (21361002), and the Young Scientists Training Program of Jiangxi Province (20122BCB23020).

Supporting information for this article is available on the WWW under http://dx.doi.org/10.1002/anie.201408491.

Compound **1** was synthesized as block-shaped single crystals by evaporation of a solution of $Cd(NO_3)_2{\cdot}4H_2O$, NaN_3, and $[(CH_3)_2NH_2]NO_3$ (see the Supporting Information). The thermogravimetric analysis (TGA) curve shows that **1** decomposes at 363 K under a nitrogen atmosphere (see Figure S1 in the Supporting Information). According to differential scanning calorimetry (DSC) measurements, two anomalies are detected at 175/172 K during the heating/cooling processes, indicating that **1** undergoes a reversible phase transition with a small thermal hysteresis (see Figure S2). For the heat-capacity (C_p) measurement, a λ-type peak is detected at around 174 K (Figure 1). The ΔC_P and

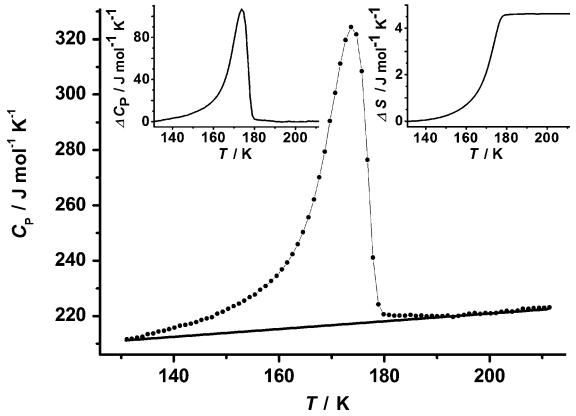

Figure 1. Heat capacity measurement for **1**. Inset: the ΔC_P (left) and ΔS values (right) related to the phase transition as a function of temperature.

ΔS values related to the phase transition increase gradually from 130 K to 160 K. With a further increase in temperature, ΔC_P exhibits a sharp peak at 174 K, whereas the ΔS value exhibits a sharp increase followed by a plateau at above 179 K. The dependence of ΔC_P and ΔS values on temperature suggest that the phase transition has a first-order character.

To understand the structural phase transition, in situ single-crystal variable-temperature X-ray diffraction was performed for **1**. It reveals that **1** crystallizes in the space group $P\bar{1}$ at 150 K (labeled as the α phase) and in $R\bar{3}$ at 203/273 K (labeled as the β phase), respectively (Table S1). The crystal structures in both phases can be roughly described as a distorted perovskite-like structure (Figure 2). The Cd^{II} ion is octahedrally coordinated by six N atoms from six azido ions, all of which act as end-to-end bridging ligands between two Cd^{II} ions, thus leading to a three-dimensional cage-like host framework. The common structural feature of **1** is the anionic $[Cd(N_3)_3]^-$ cage unit enclosed by twelve Cd–N–N–N–Cd fragments, within which the guest $[(CH_3)_2NH_2]^+$ ion resides.

The structural difference between the α and β phases can mainly be attributed to the different motion modes of the $[(CH_3)_2NH_2]^+$ guest as well as a distinguishable deformation of the $[Cd(N_3)_3]^-$ framework, which leads to the structural phase transition. In the α phase, there is one unique Cd^{II} ion and three types of crystallographically independent N_3^- ligands in the $[Cd(N_3)_3]^-$ framework, each of which (including metal and ligands) is half-occupied and located at

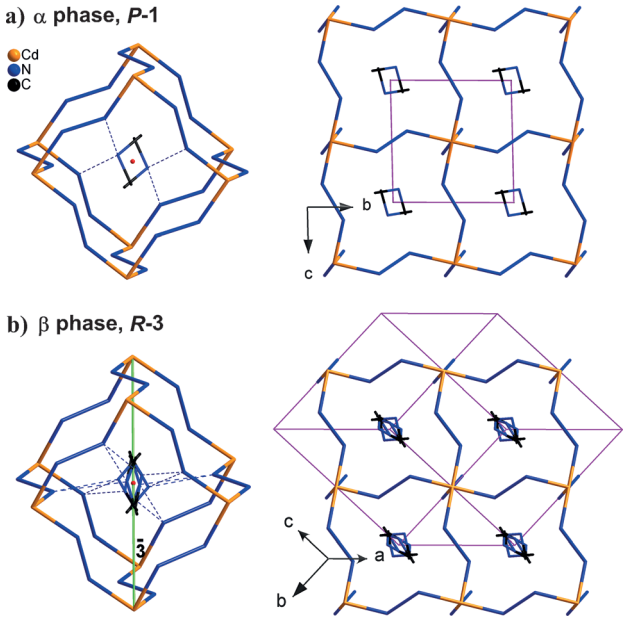

Figure 2. Cage unit and packing diagrams of **1** at a) 150 K (α phase) and b) 203 K (β phase). The dimethyl ammonium cation is disordered over two sites in the α phase and over six sites in the β phase. Hydrogen bonds are represented by dashed lines and H atoms are omitted for clarity.

an inverse center. In the β phase, the unique Cd^{II} ion is located on a $\bar{3}$ center with the occupancy decreased to one sixth. The site of the N_3^- ligand itself is also related by an inverse center, but the number of crystallographically independent N_3^- ligands decreases from three halves to one half. Although the Cd···Cd bond lengths within a $[Cd(N_3)_3]^-$ cage unit change very slightly in the two phases, the Cd···Cd···Cd angles vary remarkably (Figure S3), implying that the $[Cd(N_3)_3]^-$ framework has a remarkable deformability. More importantly, such deformability can lead to the variety of symmetry elements found for the $[Cd(N_3)_3]^-$ framework, which essentially triggers the structural phase transition. On the other hand, the $[(CH_3)_2NH_2]^+$ guests in both phases rotate dynamically but show different degrees of disorder. In the α phase, the $[(CH_3)_2NH_2]^+$ guest exhibits twofold disorder related by an inverse center, whereas in the β phase it features sixfold disorder related by a $\bar{3}$ center, as required by the imposed trigonal $R\bar{3}$ symmetry. It should also be noted that although the guest cation is disordered, hydrogen-bonding interactions can be found between the $[(CH_3)_2NH_2]^+$ guest and the nitrogen atoms of the host $[Cd(N_3)_3]^-$ framework in both phases (Figure 2, Table S3).

During the β→α phase, the symmetry of the system is broken (Figure S4)[20] with a total symmetry decrease from six symmetric elements (E, $2C_3$, i, $2S_6$) to two (E, i). Thus, this phase transition is ferroelastic with three equivalent ferroelastic directions and has an Aizu notation of $\bar{3}F\bar{1}$.[21] According to the Curie symmetry principle, the space group in the ferroelastic phase should be the subspace group in the paraelastic phase, that is, one set of its maximal non-isomorphic subgroups contain $R3$ and $P\bar{1}$. Overall, the ferroelastic phase transition is characterized by a change in

the crystal system and the related lattice distortion is shown by the spontaneous strain accompanying such a transition.[22] The driving force for the ferroelastic phase transition α↔β is thought to be mainly the deformation of the $[Cd(N_3)_3]^-$ framework and the simultaneous change in the rotation modes of the $[(CH_3)_2NH_2]^+$ guest. For an order–disorder transition, $\Delta S = R\ln(N)$, where R is the gas constant and N is the ratio of the numbers of respective geometrically distinguishable orientations in both phases. According to the X-ray diffraction studies on the two/sixfold disordered $[(CH_3)_2NH_2]^+$ ions, the theoretical value of N should be 3 and thus the calculated ΔS value should be 9.1 $J\,K^{-1}\,mol^{-1}$. However, from the C_P measurement, the ΔS value for this phase transition can be estimated to be 4.6 $J\,K^{-1}\,mol^{-1}$, which is about half of the expected value. This result shows that there is some residual entropy, implying that the phase transition has some relaxor character.[23]

Furthermore, the dynamic rotation of the guest cation and the relaxor character of such a phase transition were further demonstrated by variable-temperature dielectric spectroscopy. As shown in Figure 3, the temperature-dependent complex dielectric permittivity ($\varepsilon = \varepsilon' - i\varepsilon''$) was measured over a broad range from 0.5 to 1000 kHz and could be clearly

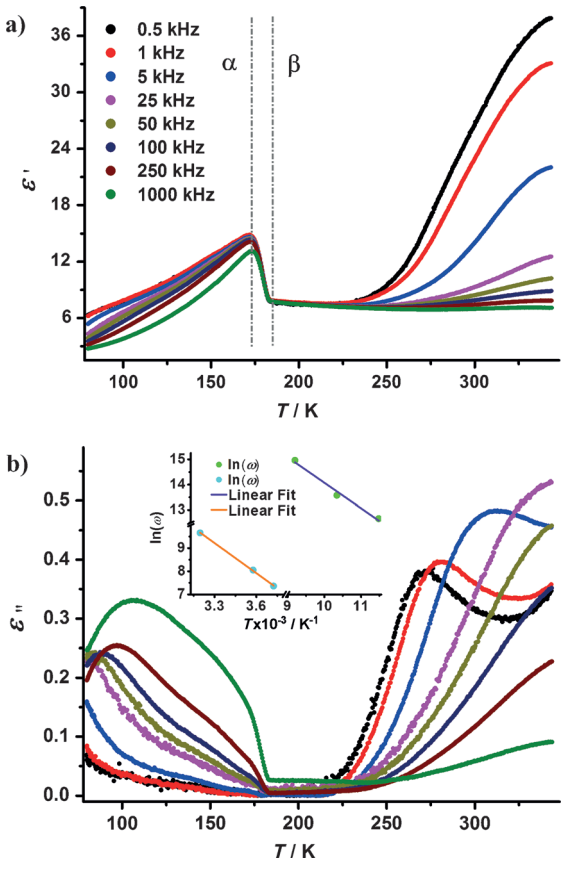

Figure 3. Temperature-dependent measurement of a) ε' and b) ε'' at various ac frequencies for a powder-pressed pellet sample of **1**. Inset in (b): Arrhenius representation of the data providing the linear fitting of $\ln(\omega)$ versus $1000/T_{peak}$ for the ferroelastic phase (denoted by green circles and the blue fitted line) and the paraelastic phase (blue circles and orange fitted line).

divided into three regions: ferroelastic, paraelastic, and phase-transition regions.

In the ferroelastic region, the real part (ε') of the complex dielectric constant increased steadily from 80 K to circa 173 K under all measured frequencies. For example, at 1000 kHz the ε' value increased from 2.7 at 80 K to 13.2 at 173 K. At this temperature the ε' value is slightly frequency dependent, suggesting the dynamic feature of a polar rotator in **1**.[24–27] The relaxation process can be clearly demonstrated by the frequency dependence of the ε'' value, in which ε'' peak maxima were found at peak temperatures (T_{peak}) of 109, 97, and 87 K for $\nu = 1000$, 250, and 100 kHz, respectively.

Based on the Debye-type relaxation process, the relationship between the ε'' value and temperature (T) can be expressed as: $\varepsilon''(T) = \omega\tau(T)/[1+\omega^2\tau(T)^2]$, where ω is the angular frequency of the test field and $\tau(T)$ is the relaxation time. The term $\tau(T)$ is a function of temperature in accordance with the Arrhenius law: $1/\tau = \omega_0 \exp[-E_a/(k_B T)]$, where E_a is the activation energy, ω_0 is a pre-exponential factor, and k_B is the Boltzmann constant. The ε'' value reaches a maximum when $\omega\tau(T) = 1$. Thus, the test frequency can be used to estimate the rotational rate ($1/\tau$) at T_{peak}, and based on this a ω_0 value of $3.13 \times 10^{10}\ s^{-1}$ and an E_a value of 2.00 kcal mol^{-1} were obtained from the plot of $1000/T_{peak}$ versus $\ln(\omega)$ for the ferroelastic phase (Figure 3b, inset).

In the paraelastic region, the dielectric relaxation behavior was significantly different to that detected in the ferroelastic phase, implying a different relaxation process. Based on the frequency dependence of the ε'' value, in which maximum peak temperatures (T_{peak}) were found at 269, 280, and 313 K for $\nu = 0.5$, 1, and 5 kHz, respectively, ω_0 and E_a values were estimated as $1.73 \times 10^{10}\ s^{-1}$ and 8.64 kcal mol^{-1}, respectively, for the paraelastic phase (Figure 3b, inset). The ω_0 value for the paraelastic phase is about half that of the ferroelastic region, whereas the E_a value is significantly increased, indicating that the polar $[(CH_3)_2NH_2]^+$ ion is more strongly confined by the host framework in the paraelastic phase. Additionally, it should be noted that the slight increase in ε'' values at temperatures above 330 K is due to an increase in the conductivity at high temperatures.[26]

During the phase-transition process, the dielectric constant shows a sharp decline at around the transition temperature (T_c), for example the ε' value at 1000 kHz decreased from 22.2 at 174 K to 13.3 at 183 K. From the structural data at 150 K and 203 K, the net orientation dipole moment in each cage was estimated to be circa 4.9 and 4.7 Debye, respectively (see Supporting Information). Therefore, the significant decrease of the dielectric constant at this stage is most likely not caused by the slight change of the net dipole moment but should be mainly ascribed to the significant increase of activation energy from 2.00 kcal mol^{-1} at the ferroelastic phase to 8.64 kcal mol^{-1} at the paraelastic phase. The rotation dynamics of the $[(CH_3)_2NH_2]^+$ ions are mostly controlled by the confinement effect, including steric effects and hydrogen-bonding interactions, of the anionic cage walls of the deformable coordination framework. The deformation of the host framework during the phase transition results in two different confinement effects for the guest cations, which is somewhat weak in $P\bar{1}$ ferroelastic phase and much stronger

in the $R\bar{3}$ paraelastic phase. Thus, the reorientation motions of the cations in the low-temperature ferroelastic phase are surprisingly much faster than those in the high-temperature paraelastic phase.

By and large, the dielectric measurements show rarely observed two-stage switchable dielectric relaxations, revealing that the molecular dynamics of the polar cation guest are well controlled by the variable confined space of the host framework, with a remarkable increase of the rotational energy barrier from the ferroelastic to the paraelastic phase. As a result, upon heating starting at low temperature, **1** shows a notable switch from a low to a high dielectric state[28] at all measured frequencies of the ferroelastic phase. With continued heating, **1** then switches again to a low dielectric state during the phase transition. Thus, **1** serves as a model sensitive thermoresponsive dielectric material over a broad range of frequencies, especially in the low-temperature ferroelastic phase.

Considering recent studies by Zhang and co-workers on the molecular dynamics of the $[(CH_3)_2NH_2]^+$ ion in a confined space constructed by the double-perovskite-like $[KCo(CN)_6]^{2-}$ framework,[11c] we proposed two possible rotation models for the ferroelastic and paraelastic phases, respectively (Figure 4). In both models, a 180° flip about the

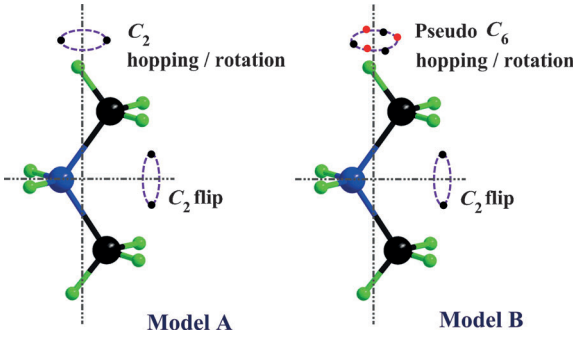

Figure 4. Proposed rotation models for the dimethyl ammonium cation in the ferroelastic (model A) and paraelastic phases (model B) of **1**.

electric-dipole C_2 axis does not change the orientation of the dipole moment and should be thus dielectrically inactive. In contrast, rotation about the axis perpendicular to the dipole C_2 axis of the cation, specifically the C_2 axis in model A and the pseudo-C_6 axis in model B, respectively, changes the orientation of the dipole moment and is thus dielectrically active. Moreover, the dielectrically active molecular dynamics of $[(CH_3)_2NH_2]^+$ ions are well confined by the anionic $[Cd(N_3)_3]^-$ framework through supramolecular interactions in **1**, such as ionic interactions and hydrogen bonding. Confinement leads to the remarkable dielectric relaxation behavior detected over a broad frequency range. This behavior is absent in $[(CH_3)_2NH_2][KCo(CN)_6]$ because no evident hydrogen-bonding interaction occurs between $[(CH_3)_2NH_2]^+$ ions and the $[KCo(CN)_6]^{2-}$ framework.

It is also meaningful to compare **1** with its Mn^{II} analogue, $[(CH_3)_2NH_2][Mn(N_3)_3]$, which was recently reported by Wang and co-workers.[19] In contrast to **1** which undergoes a ferroelastic phase transition of $P\bar{1}\leftrightarrow R\bar{3}$, the Mn^{II} analogue exhibits a non-ferroelastic phase transition of $P2_1\leftrightarrow Cmca$, and the transition temperature (T_c) is about 115 K higher than that of **1**. It is surprising that although the lengths of Cd–N bonds are slightly longer than those of Mn–N bonds, the Cd···Cd distances in the $[Cd(N_3)_3]^-$ cage unit are slightly shorter than the Mn···Mn distances, implying that **1** has a more flexible framework than its Mn^{II} analogue. This phenomenon may be ascribed to a slightly larger ionic radius and a more easily distorted coordination environment for the Cd^{II} ion. Moreover, although hydrogen-bonding interactions also occur in the Mn^{II} analogue, the change of dielectric constants before and after the phase transition, $\Delta\varepsilon' < 0.2$ at 1000 kHz, is much less than that in **1** ($\Delta\varepsilon' \approx -8.9$ at 1000 kHz). These two isostructural compounds differ only in the metal component but show distinctly different phase-transition behaviors and dielectric responses, showing that subtle changes in the coordination parameters can modulate the flexibility of the perovskite-like azido framework to tune its structural phase-transition behavior and the related physical properties.

In summary, a perovskite-like coordination polymer composed of a deformable framework embedded with polar cations **1** has been synthesized and studied by the combined techniques of variable-temperature single-crystal X-ray diffraction and dielectric measurements. **1** undergoes a reversible ferroelastic phase transition because of the varied motion modes of the $[(CH_3)_2NH_2]^+$ guest accompanied by a synergistic deformation of the $[Cd(N_3)_3]^-$ framework. The guest molecular dynamics of the polar cation are controlled by the variable confined space of the host framework, with a remarkable change of the rotational energy barrier from a ferroelastic to a paraelastic phase. Investigations on such a thermoresponsive host–guest system may be key to understanding and modulating the molecular/ionic dynamics of guest molecules in various confined spaces and may afford a useful strategy to search for new sensitive thermoresponsive dielectric materials.

Received: August 24, 2014
Published online: November 27, 2014

Keywords: dielectric materials · host–guest systems · inclusion compounds · molecular dynamics · phase transitions

[1] A. Müller, H. Reuter, S. Dillinger, *Angew. Chem. Int. Ed. Engl.* **1995**, *34*, 2328–2361; *Angew. Chem.* **1995**, *107*, 2505–2539.
[2] *Host-Guest Systems Based on Nanoporous Crystals* (Eds.: F. Laeri, F. Schüth, U. Simon, M. Wark), Wiley-VCH, Weinheim, **2003**.
[3] E. R. Kay, D. A. Leigh, F. Zerbetto, *Angew. Chem. Int. Ed.* **2007**, *46*, 72–191; *Angew. Chem.* **2007**, *119*, 72–196.
[4] G. Férey, C. Serre, *Chem. Soc. Rev.* **2009**, *38*, 1380–1399.
[5] X. Yan, F. Wang, B. Zheng, F. Huang, *Chem. Soc. Rev.* **2012**, *41*, 6042–6065.
[6] T. Ogoshi, K. Kida, T. Yamagishi, *J. Am. Chem. Soc.* **2012**, *134*, 20146–20150.
[7] Y. Zhang, H.-Y. Ye, D.-W. Fu, R.-G. Xiong, *Angew. Chem. Int. Ed.* **2014**, *53*, 2114–2118; *Angew. Chem.* **2014**, *126*, 2146–2150.
[8] F. Huang, L. Isaacs, *Acc. Chem. Res.* **2014**, *47*, 1923–1924.

[9] Z. Wang, B. Zhang, T. Otsuka, K. Inoue, H. Kobayashi, M. Kurmoo, *Dalton Trans.* **2004**, 2209 – 2216.
[10] a) P. Jain, N. S. Dalal, B. H. Toby, H. W. Kroto, A. K. Cheetham, *J. Am. Chem. Soc.* **2008**, *130*, 10450 – 10451; b) W. Li, A. Thirumurugan, P. T. Barton, Z. Lin, S. Henke, H. H.-M. Yeung, M. T. Wharmby, E. G. Bithell, C. J. Howard, A. K. Cheetham, *J. Am. Chem. Soc.* **2014**, *136*, 7801 – 7804.
[11] a) W. Zhang, Y. Cai, R.-G. Xiong, H. Yoshikawa, K. Awaga, *Angew. Chem. Int. Ed.* **2010**, *49*, 6608 – 6610; *Angew. Chem.* **2010**, *122*, 6758 – 6760; b) D.-W. Fu, W. Zhang, H.-L. Cai, Y. Zhang, R.-G. Xiong, S. D. Huang, T. Nakamura, *Angew. Chem. Int. Ed.* **2011**, *50*, 11947 – 11951; *Angew. Chem.* **2011**, *123*, 12153 – 12157; c) W. Zhang, H.-Y. Ye, R. Graf, H. W. Spiess, Y.-F. Yao, R.-Q. Zhu, R.-G. Xiong, *J. Am. Chem. Soc.* **2013**, *135*, 5230 – 5233.
[12] Y. Takahashi, R. Obara, Z.-Z. Lin, Y. Takahashi, T. Naito, T. Inabe, S. Ishibashi, K. Terakura, *Dalton Trans.* **2011**, *40*, 5563 – 5568.
[13] T. Asaji, Y. Ito, J. Seliger, V. Žagar, A. Gradišek, T. Apih, *J. Phys. Chem. A* **2012**, *116*, 12422 – 12428.
[14] a) M. Maczka, A. Pietraszko, B. Macalik, K. Hermanowicz, *Inorg. Chem.* **2014**, *53*, 787 – 794; b) M. Mączka, A. Ciupa, A. Gągor, A. Sieradzki, A. Pikul, B. Macalik, M. Drozd, *Inorg. Chem.* **2014**, *53*, 5260 – 5268.
[15] A. Kojima, K. Teshima, Y. Shirai, T. Miyasaka, *J. Am. Chem. Soc.* **2009**, *131*, 6050 – 6051.
[16] S. Kazim, M. K. Nazeeruddin, M. K. Nazeeruddin, M. Grätzel, S. Ahmad, *Angew. Chem. Int. Ed.* **2014**, *53*, 2812 – 2824; *Angew. Chem.* **2014**, *126*, 2854 – 2867.
[17] a) Z.-Y. Du, Y.-P. Zhao, W.-X. Zhang, H.-L. Zhou, C.-T. He, W. Xue, B.-Y. Wang, X.-M. Chen, *Chem. Commun.* **2014**, *50*, 1989 – 1991; b) Z.-Y. Du, Y.-P. Zhao, C.-T. He, B.-Y. Wang, W. Xue, H.-L. Zhou, J. Bai, B. Huang, W.-X. Zhang, X.-M. Chen, *Cryst. Growth Des.* **2014**, *14*, 3903 – 3909.
[18] a) F. A. Mautner, H. Krischner, C. Kratky, *Monatsh. Chem.* **1988**, *119*, 1245 – 1249; b) F. A. Mautner, R. Cortes, L. Lezama, T. Rojo, *Angew. Chem. Int. Ed. Engl.* **1996**, *35*, 78 – 80; *Angew. Chem.* **1996**, *108*, 96 – 98; c) S. Hanna, F. A. Mautner, B. Koppelhuber-Bitschnau, M. A. M. Abu-Youssef, *Mater. Sci. Forum* **2000**, *321 – 324*, 1098 – 1101.
[19] X.-H. Zhao, X.-C. Huang, S.-L. Zhang, D. Shao, H.-Y. Wei, X.-Y. Wang, *J. Am. Chem. Soc.* **2013**, *135*, 16006 – 16009.
[20] *International tables for crystallography*, *Vol. A*, *5th ed.*, (Ed.: T. Hahn), Springer, Dordrecht, Netherlands, **2002**.
[21] As one kind of ferroic behavior, ferroelasticity is defined by a strain–stress hysteresis. As it is very difficult to measure ferroelastic hysteresis with any acceptable degree of accuracy, it has become customary to call a material "ferroelastic" if a phase transition occurs which may conceivably generate ferroelasticity. Theoretically, such phase transitions should belong to the 94 species which are deduced by Aizu. For details, see: a) K. Aizu, *J. Phys. Soc. Jpn.* **1969**, *27*, 387 – 396; b) E. K. H. Salje, *Contemp. Phys.* **2000**, *41*, 79 – 91.
[22] V. K. Wadhawan, *Bull. Mater. Sci.* **1984**, *6*, 733 – 753.
[23] a) R. Samantaray, R. J. Clark, E. S. Choi, H. Zhou, N. S. Dalal, *J. Am. Chem. Soc.* **2011**, *133*, 3792 – 3795; b) R. Samantaray, R. J. Clark, E. S. Choi, N. S. Dalal, *J. Am. Chem. Soc.* **2012**, *134*, 15953 – 15962.
[24] *Broadband Dielectric Spectroscopy* (Eds.: F. Kremer, A. Schönhals), Springer, Berlin, **2002**.
[25] S. Devautour-Vinot, G. Maurin, C. Serre, P. Horcajada, D. Paula da Cunha, V. Guillerm, E. de Souza Costa, F. Taulelle, C. Martineau, *Chem. Mater.* **2012**, *24*, 2168 – 2177.
[26] Q.-C. Zhang, F.-T. Wu, H.-M. Hao, H. Xu, H.-X. Zhao, L.-S. Long, R.-B. Huang, L.-S. Zheng, *Angew. Chem. Int. Ed.* **2013**, *52*, 12602 – 12605; *Angew. Chem.* **2013**, *125*, 12834 – 12837.
[27] P. Sippel, D. Denysenko, A. Loidl, P. Lunkenheimer, G. Sastre, D. Volkmer, *Adv. Funct. Mater.* **2014**, *24*, 3885 – 3896.
[28] The silicon nitride, with $\varepsilon' \approx 7$, is often viewed as the typical boundary between high and low dielectric constant materials, both of which are useful for different applications. For related references, see: a) P. Simon, Y. Gogotsi, *Nat. Mater.* **2008**, *7*, 845 – 854; b) P. A. Kohl, *Annu. Rev. Chem. Biomol. Eng.* **2011**, *2*, 379 – 401.

